Metal–Organic Frameworks

How to cite:
International Edition: doi.org/10.1002/anie.202004697
German Edition: doi.org/10.1002/ange.202004697

Isoreticular Linker Substitution in Conductive Metal–Organic Frameworks with Through-Space Transport Pathways

*Lilia S. Xie[+], Sarah S. Park[+], Michał J. Chmielewski, Hanyu Liu, Ruby A. Kharod, Luming Yang, Michael G. Campbell, and Mircea Dincă**

Abstract: *The extension of reticular chemistry concepts to electrically conductive three-dimensional metal–organic frameworks (MOFs) has been challenging, particularly for cases in which strong interactions between electroactive linkers create the charge transport pathways. Here, we report the successful replacement of tetrathiafulvalene (TTF) with a nickel glyoximate core in a family of isostructural conductive MOFs with Mn^{2+}, Zn^{2+}, and Cd^{2+}. Different coordination environments of the framework metals lead to variations in the linker stacking geometries and optical properties. Single-crystal conductivity data are consistent with charge transport along the linker stacking direction, with conductivity values only slightly lower than those reported for the analogous TTF materials. These results serve as a case study demonstrating how reticular chemistry design principles can be extended to conductive frameworks with significant intermolecular contacts.*

Electrically conductive metal–organic frameworks (MOFs) are a promising class of porous conductors.[1,2] They are appealing for applications benefitting from facile charge transport and high surface area, including chemiresistive sensing,[3–6] electrochemical energy storage,[7–11] and electrocatalysis.[12–14] Many conductive MOFs have incorporated building blocks from molecular organic conductors into frameworks.[15–21] Although a diverse library of ligands exists, techniques to regulate the spatial arrangement of electroactive units are less developed.[22–24] Since electronic coupling among linkers often facilitates charge transport, synthetic control over stacking interactions would enable conductive MOFs with tailored structures and transport properties.

Many studies of linker stacking interactions in conductive MOFs have focused on the tetrathiafulvalene tetrabenzoate (TTFTB) linker.[16,22,23,25–27] These materials exhibit a variety of stacking arrangements involving the tetrathiafulvalene (TTF) cores, with close and continuous stacking correlating with the highest conductivities (up to 10^{-4} S cm^{-1}).[22,23,27] Importantly, a comparative analysis of MOFs with tetratopic carboxylate linkers indicated that TTFTB frameworks tend to exhibit unique topologies due to this linker's propensity for π–π interactions and structural flexibility.[23] These characteristics are responsible for the interesting electronic properties, but also hinder translation of design strategies from TTFTB-based MOFs to other linkers. Extending the scope of reticular chemistry—that is, the controlled assembly of frameworks based on conserved secondary building units (SBUs)[28]—to include structures with pronounced intermolecular interactions is hence an unmet need.[29]

Complexes of nickel(II) with glyoximate ligands have been known for more than a century,[30] and have been employed for analytical determination of nickel content.[31] Like TTF derivatives,[32] they stack extensively in the solid state[33] and form conductive charge transfer salts.[34] Therefore, we hypothesized that a tetratopic linker with a nickel glyoximate core would behave similarly to TTFTB. Here, we present a new metallolinker, nickel(II) bis(dibenzoateglyoximate) ($Ni(dbg)_2$), and show that it forms frameworks with Mn^{2+}, Zn^{2+}, and Cd^{2+} exhibiting the same topology as the corresponding TTFTB MOFs. These structures contain helical linker stacks with Ni···Ni distances as close as 3.70 Å, resulting in electrical conductivities up to 10^{-6} S cm^{-1}. These results demonstrate a novel instance of isoreticular substitution of linkers in MOFs with through-space transport pathways.

The $H_4Ni(dbg)_2$ linker was synthesized by metalation of the glyoxime dibenzoic acid (dbg) ligand (Scheme 1), which was obtained via benzoin condensation of methyl 4-formylbenzoate and subsequent oxidation and treatment with hydroxylamine (Scheme S1 and Figures S1–S10; a cobaloxime MOF linker was recently obtained using a similar route[35]). Combining $H_4Ni(dbg)_2$ with $Mn(NO_3)_2{\cdot}4H_2O$, $Zn(NO_3)_2{\cdot}6H_2O$, and $Cd(NO_3)_2{\cdot}4H_2O$ under solvothermal reaction conditions mimicking those used for the M_2(TTFTB) MOFs[16,22] led to the isolation of $Mn_2[Ni(dbg)_2]$ (**Mn**), $Zn_2[Ni(dbg)_2]$ (**Zn**), and $Cd_2[Ni(dbg)_2]$ (**Cd**).

Single-crystal X-ray diffraction (SCXRD) showed all three phases are isostructural to one another and to the

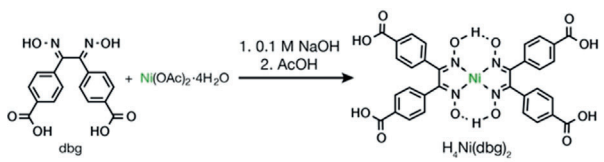

Scheme 1. Synthesis of $H_4Ni(dbg)_2$.

[*] L. S. Xie,[+] Dr. S. S. Park,[+] Dr. M. J. Chmielewski, H. Liu, R. A. Kharod, L. Yang, Dr. M. G. Campbell, Prof. M. Dincă
Department of Chemistry, Massachusetts Institute of Technology
77 Massachusetts Avenue, Cambridge, MA 02139 (USA)
E-mail: mdinca@mit.edu
Dr. M. J. Chmielewski
Faculty of Chemistry, Biological and Chemical Research Centre, University of Warsaw
Żwirki i Wigury 101, 02-089 Warszawa (Poland)
[+] These authors contributed equally to this work.
Supporting information and the ORCID identification number(s) for the author(s) of this article can be found under https://doi.org/10.1002/anie.202004697.

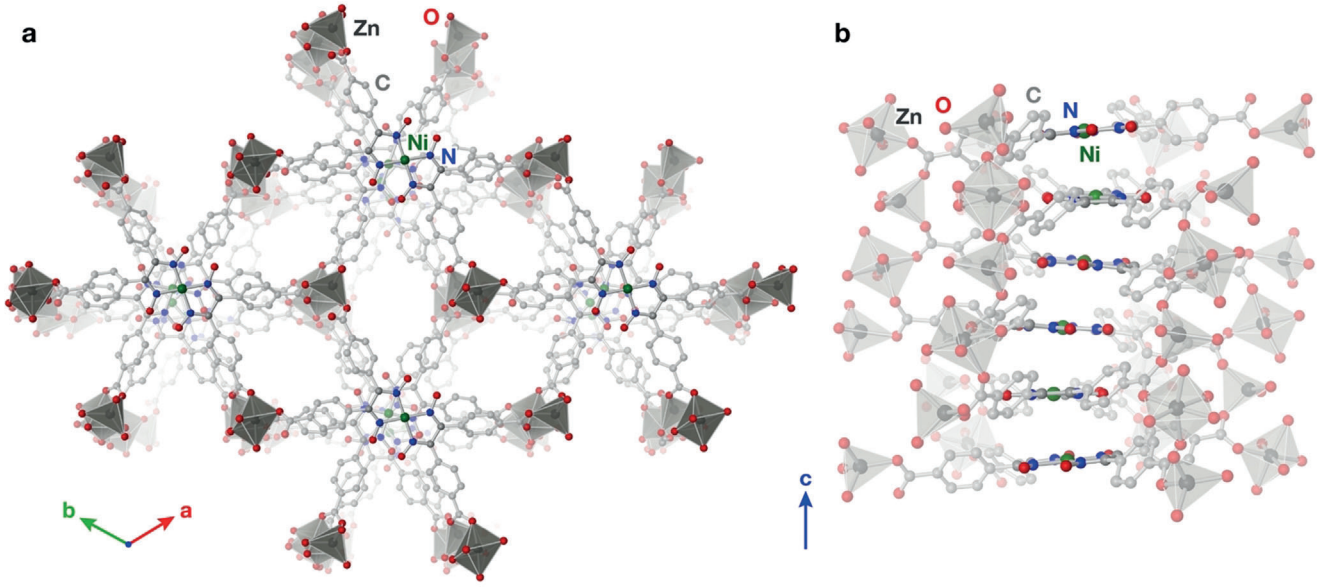

Figure 1. Portions of the crystal structure of **Zn**, viewed a) along the *c* axis, showing rhombic pores, and b) perpendicular to the *c* axis, showing helical stacking of nickel glyoximate cores. Hydrogen atoms are omitted for clarity.

M_2(TTFTB) MOFs, with **Mn** and **Cd** crystallizing in space groups $P6_5/P6_1$, and **Zn** in space groups $P6_522/P6_122$ (Tables S1–S3 and Figures S11–S13). (The measured crystals of **Mn** and **Cd** exhibited inversion twinning, suggesting that the products are not enantiopure.) In each phase, the linkers form helical stacks along the *c* axis (Figure 1). The framework metal atoms are coordinated by linker carboxylates and solvent atoms to form one-dimensional (1D) inorganic SBUs. Rhombic 1D pores also extend along the *c* direction. Nitrogen adsorption isotherms of activated **Mn**, **Zn**, and **Cd** revealed them to be permanently porous, with Brunauer–Emmett–Teller (BET) surface areas of 543.2(3), 539.8(4), and 486.7(5) $m^2 g^{-1}$, respectively (Figures S13–S19), similar to the M_2(TTFTB) materials.[16,22]

Searches of the Cambridge Structural Database[36] for entries in space groups $P6_1$, $P6_5$, $P6_122$, and $P6_522$ showed that these $M_2[Ni(dbg)_2]$ phases (and the isostructural M_2(TTFTB) MOFs) are topologically unique among polymeric extended structures. The lack of other MOFs with this topology is consistent with evidence that the geometry and π–π stacking of TTFTB are uncommon among tetratopic linkers.[23,26,29] Closely matched geometries and stacking propensities appear to enable the isoreticular substitution of $Ni(dbg)_2$ for TTFTB.

The pronounced stacking of nickel glyoximate complexes often leads to anisotropic optical and electronic properties.[37,38] Hence, we sought to further quantify the stacking geometries in these MOFs (Figure 2). Each nickel glyoximate core is nearly planar, with < 0.1 Å deviation of all atoms from the least-squares plane (Tables S4–S6). The separation between adjacent least-squares planes is slightly longer for **Mn** than **Zn** and **Cd** (Table 1). Because the $Ni(dbg)_2$ ligands are not exactly centered on the six-fold screw axes, the Ni···Ni distances are longer than the interplanar spacings. These contact distances are similar to the S···S distances observed in the M_2(TTFTB) analogs (3.65–3.77 Å), and 0.1–0.6 Å longer than Ni···Ni distances in other nickel glyoximate complexes.[37] The slip distances between adjacent cores (defined as the magnitude of the projection of the Ni···Ni vector onto the least-squares plane) are shortest for **Zn** and longest for **Cd**.

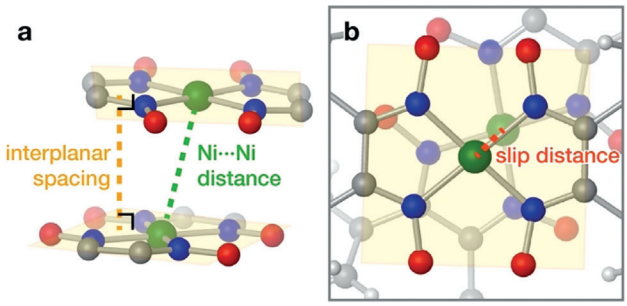

Figure 2. a) Illustration of the interplanar and Ni···Ni distances between adjacent $Ni(dbg)_2$ linkers, with the least-squares planes shown in transparent yellow. b) Illustration of the slip distance, defined as the projection of the Ni···Ni vector onto the least-squares plane.

Table 1: Crystallographic linker stacking distances in $M_2[Ni(dbg)_2]$ MOFs.

MOF	Interplanar [Å]	Ni···Ni [Å]	Slip [Å]
Mn	3.6663	3.8131(9)	1.0480(2)
Zn	3.5767	3.7027(6)	0.9582(2)
Cd	3.5887	3.7704(11)	1.1566(3)

Distinctions in the linker stacking geometries can be explained by the different coordination environments of the metal centers in the inorganic SBUs. In each phase, two crystallographically independent framework M^{2+} centers coordinated by linker carboxylates and solvent oxygen atoms form continuous 1D SBUs encircling the three-fold screw axis (Figure 3). The five-coordinate Mn^{2+} centers in **Mn** form corner-sharing polyhedra that pack relatively inefficiently, resulting in the longest interplanar spacing. In **Zn**, the

alternating tetrahedra and pseudo-octahedra do not share any oxygen atoms. The small ionic radius of Zn^{2+} coupled with a relatively straight SBU results in the shortest interplanar, Ni···Ni, and slip distances.[39] Finally, the Cd^{2+} centers in **Cd** form edge-sharing polyhedra that effectively compress the pitch of the linker stacking helix while increasing its diameter compared to **Mn** and **Zn**. As a result, the interplanar spacing of **Cd** is similar to **Zn**, while the slip distance is the largest among the three phases.

Because stacking often influences the electronic transitions of d^8 square planar complexes in the solid state,[40] we examined the diffuse reflectance UV-visible (DRUV-vis) spectra of **Mn**, **Zn**, and **Cd** (Figure 4). Bands in the region 30000 to 40000 cm^{-1} are likely transitions with predominantly $\pi \rightarrow \pi^*$ character from the dbg ligand (Figure S20).[38] Bands between 22000 and 28000 cm^{-1} are assigned to metal-to-ligand charge transfer (MLCT) transitions from Ni 3d orbitals to states with π^* character.[38,41] All of these features are present in the solution-phase absorbance spectrum of $H_4Ni(dbg)_2$, with the bands blue-shifted by 1000–3000 cm^{-1} compared to the MOFs.

Bands between 16000 and 22000 cm^{-1} are present in all of the solid-state MOF spectra, but absent from the solution-phase linker spectrum. We tentatively assign these features to transitions originating from filled Ni 3d orbitals to the empty Ni $4p_z$ orbitals. Closer Ni···Ni distances result in red-shifted bands in this region for nickel glyoximate complexes.[37,38,42] The presence of these features in the MOF spectra and their absence in the solution-phase spectrum of $H_4Ni(dbg)_2$ are consistent with previous suggestions that the $3d_{z^2} \rightarrow 4p_z$ transition is intensified by mixing with interatomic charge transfer interactions in the solid state.[41] The more intense features in **Zn** and **Cd** likely correlate with their closer Ni···Ni distances and interplanar spacings compared to **Mn**.

Motivated by the structural analogy to the conductive M_2(TTFTB) MOFs and the precedent of stacking-dependent transport properties in nickel glyoximate complexes,[43] we

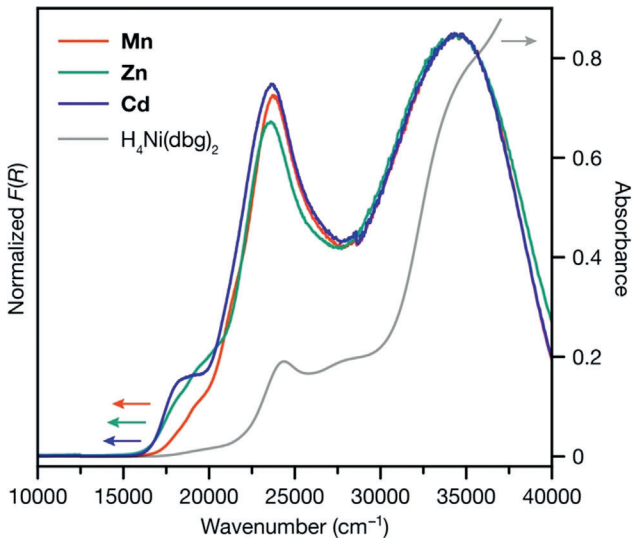

Figure 3. Kubelka–Munk-transformed diffuse reflectance UV-visible spectra of **Mn**, **Zn**, and **Cd**, and absorption spectrum of a 0.025 mM solution of $H_4Ni(dbg)_2$ in DMF.

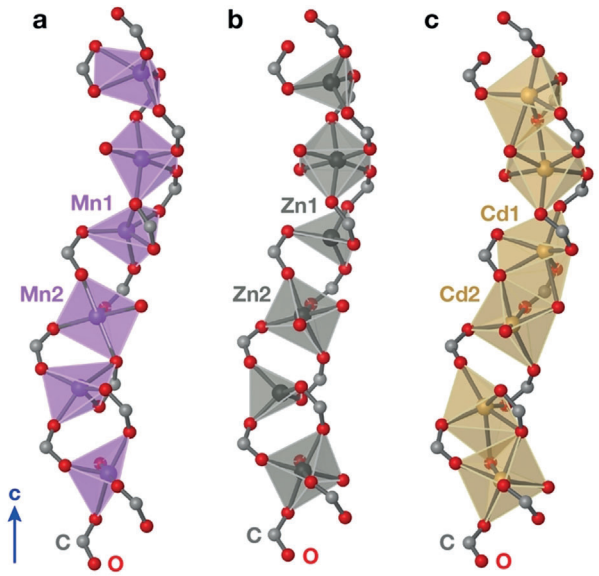

Figure 4. Different coordination environments in the inorganic secondary building units of a) **Mn**, b) **Zn**, and c) **Cd**, which comprise carboxylate-bridged chains of metal centers.

investigated the electrical conductivities of **Mn**, **Zn**, and **Cd**. Two-contact probe single-crystal devices of **Mn** and **Cd** (Figures S21 and S22) revealed champion conductivity values of 2.0×10^{-7} S cm^{-1} for **Mn** and 2.7×10^{-6} S cm^{-1} for **Cd** along the stacking direction (Tables S7 and S8). These values are about 2–3 orders of magnitude lower than the TTFTB analogs,[22] but higher than neutral nickel glyoximate complexes with similar interplanar spacings (Table S9).[34] (Due to crystal size limitations, we were unable to carry out single-crystal measurements on **Zn**.) Two-contact probe pressed pellets yielded typical values of $< 10^{-10}$ S cm^{-1} for **Mn**, **Zn**, and **Cd** (Tables S10–S12 and Figure S23). The lower pellet conductivities are consistent with the expected anisotropic charge transport pathways. One important distinction from the M_2(TTFTB) analogs[16,22] is the lack of linker oxidation or mixed-valency in the as-synthesized $M_2[Ni(dbg)_2]$ MOFs. Neither DRUV-vis nor electron paramagnetic resonance spectroscopies exhibited signatures of radical species (Figure S24), suggesting that the somewhat inferior charge transport properties of these materials relative to their TTFTB congeners are likely due to their lower carrier concentrations. However, attempts to post-synthetically oxidatively or reductively dope these materials have not resulted in higher conductivities thus far (Figure S25 and Table S13), leading us to hypothesize that other oxidation states of the linker may not be stable in these structures.

In summary, whereas TTFTB stood out thus far in forming unique MOF topologies with strong stacking that engendered good charge transport, isoreticular substitution of TTFTB with new nickel glyoximate complexes yielded three new materials with identical topology and similar electrical properties in line with their reduced charge carrier density. This work introduces square planar metal glyoximate complexes as a metallolinker platform for MOFs in which the intermolecular arrangements of linkers delineate their optical and electronic properties. In general, further development of

isoreticular strategies for linkers exhibiting strong stacking interactions can inform the targeted design of new conductive MOFs.

Acknowledgements

This work was supported by the U.S. Department of Energy, Office of Science, Office of Basic Energy Sciences (DE-SC0018235). L.S.X. thanks the National Science Foundation for support through the Graduate Research Fellowship Program (1122374). M.J.C. thanks the Polish National Agency for Academic Exchange for Bekker fellowship. We thank Ulugbek Barotov for preliminary studies on related metallolinkers, Dr. Constanze Neumann for assistance with ICP-MS experiments, Grigorii Skorupskii for assistance with crystallography and helpful discussions, and Julius Oppenheim for insightful suggestions regarding interpretation of UV-vis data.

Conflict of interest

The authors declare no conflict of interest.

Keywords: conducting materials · glyoximes · metal–organic frameworks · reticular chemistry · stacking interactions

[1] L. Sun, M. G. Campbell, M. Dincă, *Angew. Chem. Int. Ed.* **2016**, *55*, 3566 – 3579; *Angew. Chem.* **2016**, *128*, 3628 – 3642.
[2] L. S. Xie, G. Skorupskii, M. Dincă, *Chem. Rev.* **2020**, https://doi.org/10.1021/acs.chemrev.9b00766.
[3] M. G. Campbell, D. Sheberla, S. F. Liu, T. M. Swager, M. Dincă, *Angew. Chem. Int. Ed.* **2015**, *54*, 4349 – 4352; *Angew. Chem.* **2015**, *127*, 4423 – 4426.
[4] Z. Meng, A. Aykanat, K. A. Mirica, *J. Am. Chem. Soc.* **2019**, *141*, 2046 – 2053.
[5] M. L. Aubrey, M. T. Kapelewski, J. F. Melville, J. Oktawiec, D. Presti, L. Gagliardi, J. R. Long, *J. Am. Chem. Soc.* **2019**, *141*, 5005 – 5013.
[6] I. Stassen, J.-H. Dou, C. Hendon, M. Dincă, *ACS Cent. Sci.* **2019**, *5*, 1425 – 1431.
[7] D. Sheberla, J. C. Bachman, J. S. Elias, C.-J. Sun, Y. Shao-Horn, M. Dincă, *Nat. Mater.* **2017**, *16*, 220 – 225.
[8] J. Park, M. Lee, D. Feng, Z. Huang, A. C. Hinckley, A. Yakovenko, X. Zou, Y. Cui, Z. Bao, *J. Am. Chem. Soc.* **2018**, *140*, 10315 – 10323.
[9] D. Feng, T. Lei, M. R. Lukatskaya, J. Park, Z. Huang, M. Lee, L. Shaw, S. Chen, A. A. Yakovenko, A. Kulkarni, et al., *Nat. Energy* **2018**, *3*, 30 – 36.
[10] S. S. Shinde, C. H. Lee, J.-Y. Jung, N. K. Wagh, S.-H. Kim, D.-H. Kim, C. Lin, S. U. Lee, J.-H. Lee, *Energy Environ. Sci.* **2019**, *12*, 727 – 738.
[11] K. W. Nam, S. S. Park, R. dos Reis, V. P. Dravid, H. Kim, C. A. Mirkin, J. F. Stoddart, *Nat. Commun.* **2019**, *10*, 4948.
[12] E. M. Miner, T. Fukushima, D. Sheberla, L. Sun, Y. Surendranath, M. Dincă, *Nat. Commun.* **2016**, *7*, 10942.
[13] C. A. Downes, A. J. Clough, K. Chen, J. W. Yoo, S. C. Marinescu, *ACS Appl. Mater. Interfaces* **2018**, *10*, 1719 – 1727.
[14] R. Matheu, E. Gutierrez-Puebla, M. Á. Monge, C. S. Diercks, J. Kang, M. S. Prévot, X. Pei, N. Hanikel, B. Zhang, P. Yang, et al., *J. Am. Chem. Soc.* **2019**, *141*, 17081 – 17085.
[15] S. Takaishi, M. Hosoda, T. Kajiwara, H. Miyasaka, M. Yamashita, Y. Nakanishi, Y. Kitagawa, K. Yamaguchi, A. Kobayashi, H. Kitagawa, *Inorg. Chem.* **2009**, *48*, 9048 – 9050.
[16] T. C. Narayan, T. Miyakai, S. Seki, M. Dincă, *J. Am. Chem. Soc.* **2012**, *134*, 12932 – 12935.
[17] T. Kambe, R. Sakamoto, K. Hoshiko, K. Takada, M. Miyachi, J. H. Ryu, S. Sasaki, J. Kim, K. Nakazato, M. Takata, et al., *J. Am. Chem. Soc.* **2013**, *135*, 2462 – 2465.
[18] D. Sheberla, L. Sun, M. A. Blood-Forsythe, S. Er, C. R. Wade, C. K. Brozek, A. Aspuru-Guzik, M. Dincă, *J. Am. Chem. Soc.* **2014**, *136*, 8859 – 8862.
[19] D. Chen, H. Xing, Z. Su, C. Wang, *Chem. Commun.* **2016**, *52*, 2019 – 2022.
[20] L. Qu, H. Iguchi, S. Takaishi, F. Habib, C. F. Leong, D. M. D'Alessandro, T. Yoshida, H. Abe, E. Nishibori, M. Yamashita, *J. Am. Chem. Soc.* **2019**, *141*, 6802 – 6806.
[21] H. C. Wentz, G. Skorupskii, A. B. Bonfim, J. L. Mancuso, C. H. Hendon, E. H. Oriel, G. T. Sazama, M. G. Campbell, *Chem. Sci.* **2020**, *11*, 1342 – 1346.
[22] S. S. Park, E. R. Hontz, L. Sun, C. H. Hendon, A. Walsh, T. Van Voorhis, M. Dincă, *J. Am. Chem. Soc.* **2015**, *137*, 1774 – 1777.
[23] L. S. Xie, E. V. Alexandrov, G. Skorupskii, D. M. Proserpio, M. Dincă, *Chem. Sci.* **2019**, *10*, 8558 – 8565.
[24] G. Skorupskii, B. A. Trump, T. W. Kasel, C. M. Brown, C. H. Hendon, M. Dincă, *Nat. Chem.* **2020**, *12*, 131 – 136.
[25] J. Su, T.-H. Hu, R. Murase, H.-Y. Wang, D. M. D'Alessandro, M. Kurmoo, J.-L. Zuo, *Inorg. Chem.* **2019**, *58*, 3698 – 3706.
[26] L. S. Xie, M. Dincă, *Isr. J. Chem.* **2018**, *58*, 1119 – 1122.
[27] J. Castells-Gil, S. Mañas-Valero, I. J. Vitórica-Yrezábal, D. Ananias, J. Rocha, R. Santiago, S. T. Bromley, J. J. Baldoví, E. Coronado, M. Souto, et al., *Chem. Eur. J.* **2019**, *25*, 12636 – 12643.
[28] O. M. Yaghi, M. O'Keeffe, N. W. Ockwig, H. K. Chae, M. Eddaoudi, J. Kim, *Nature* **2003**, *423*, 705 – 714.
[29] S. S. Park, C. H. Hendon, A. J. Fielding, A. Walsh, M. O'Keeffe, M. Dincă, *J. Am. Chem. Soc.* **2017**, *139*, 3619 – 3622.
[30] L. Tschugaeff, *Ber. Dtsch. Chem. Ges.* **1905**, *38*, 2520 – 2522.
[31] E. L. Bickerdike, H. H. Willard, *Anal. Chem.* **1952**, *24*, 1026.
[32] N. Martín, *Chem. Commun.* **2013**, *49*, 7025 – 7027.
[33] L. E. Godycki, R. E. Rundle, *Acta Crystallogr.* **1953**, *6*, 487 – 495.
[34] M. Cowie, A. Gleizes, G. W. Grynkewich, D. W. Kalina, R. P. Scaringe, J. A. Ibers, T. J. Marks, M. S. McClure, C. R. Kannewurf, S. L. Ruby, et al., *J. Am. Chem. Soc.* **1979**, *101*, 2921 – 2936.
[35] S. Roy, Z. Huang, A. Bhunia, A. Castner, A. K. Gupta, X. Zou, S. Ott, *J. Am. Chem. Soc.* **2019**, *141*, 15942 – 15950.
[36] C. R. Groom, I. J. Bruno, M. P. Lightfoot, S. C. Ward, *Acta Crystallogr. Sect. B* **2016**, *72*, 171 – 179.
[37] C. V. Banks, D. W. Barnum, *J. Am. Chem. Soc.* **1958**, *80*, 4767 – 4772.
[38] B. G. Anex, F. K. Krist, *J. Am. Chem. Soc.* **1967**, *89*, 6114 – 6125.
[39] R. D. Shannon, *Acta Crystallogr.* **1976**, *32*, 751 – 767.
[40] P. Day, *Inorg. Chim. Acta Rev.* **1969**, *3*, 81 – 97.
[41] Y. Ohashi, I. Hanazaki, S. Nagakura, *Inorg. Chem.* **1970**, *9*, 2551 – 2556.
[42] K. Takeda, J. Hayashi, I. Shirotani, H. Fukuda, K. Yakushi, *Mol. Cryst. Liq. Cryst.* **2006**, *460*, 131 – 144.
[43] I. Shirotani, K. Suzuki, T. Suzuki, T. Yagi, M. Tanaka, *Bull. Chem. Soc. Jpn.* **1992**, *65*, 1078 – 1083.

Manuscript received: March 31, 2020
Accepted manuscript online: April 28, 2020
Version of record online: ■■ ■■, ■■■■

Communications

Metal–Organic Frameworks

L. S. Xie, S. S. Park, M. J. Chmielewski, H. Liu, R. A. Kharod, L. Yang, M. G. Campbell, M. Dincă* ——— ■■■■–■■■■

Isoreticular Linker Substitution in Conductive Metal–Organic Frameworks with Through-Space Transport Pathways

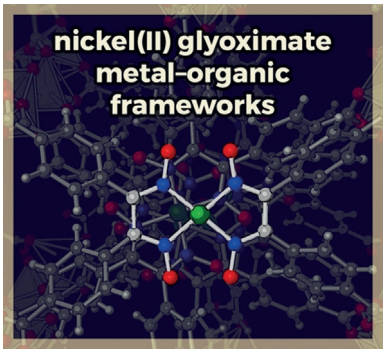

Matching the geometry and stacking propensity of linkers allows for tetrathiafulvalene to be replaced with a nickel glyoximate core in a family of metal–organic frameworks with charge transport properties that are in line with their charge density.